Characterization of plastid psbT sense and antisense RNAs

Ouafa Zghidi-Abouzid, Livia Merendino, Franck Buhr, Mustafa Malik Ghulam, Silva Lerbs-Mache

Published online 17 March 2011

Nucleic Acids Research, 2011, Vol. 39, No. 13 ***5379–5387***
doi:10.1093/nar/gkr143

Characterization of plastid *psb*T sense and antisense RNAs

Ouafa Zghidi-Abouzid, Livia Merendino, Frank Buhr, Mustafa Malik Ghulam and Silva Lerbs-Mache*

Laboratoire de Physiologie Cellulaire Végétale, UMR 5168, CNRS/UJF/INRA/CEA, CEA-Grenoble, 17 rue des Martyrs, 38054 Grenoble cedex, France

Received December 10, 2010; Revised February 23, 2011; Accepted February 24, 2011

ABSTRACT

The plastid *psb*B operon is composed of the *psb*B, *psb*T, *psb*H, *pet*B and *pet*D genes. The *psb*N gene is located in the intergenic region between *psb*T and *psb*H on the opposite DNA strand. Transcription of *psb*N is under control of sigma factor 3 (SIG3) and *psb*N read-through transcription produces antisense RNA to *psb*T mRNA. To investigate on the question of whether *psb*T gene expression might be regulated by antisense RNA, we have characterized *psb*T sense and antisense RNAs. Mapping of 5′ and 3′-ends by circular RT–PCR and /or 5′-RACE experiments reveal the existence of two different sense and antisense RNAs each, one limited to *psb*T RNA and a larger one that covers, in addition, part of the *psb*B coding region. Sense and antisense RNAs seem to form double-stranded RNA/RNA hybrids as indicated by nuclease digestion experiments followed by RT–PCR amplification to reveal nuclease resistant RNA. Western immunoblotting using antibodies made against PSBT protein and primer extension analysis of different plastid mRNA species and *psb*T antisense RNA suggest that sequestering of *psb*T mRNA by hybrid formation results in translational inactivation of the *psb*T mRNA and provides protection against nucleolytic degradation of mRNA during photo-oxydative stress conditions.

INTRODUCTION

The existence of many non-coding RNAs (ncRNAs) and different regulatory pathways mediated by antisense RNA base-pairing induced mechanisms have been discovered during the last years. Most of this work concerns eukaryotic nucleus-encoded natural antisense transcripts (NATs) and ncRNAs in bacteria (1–3). Much less is known on ncRNAs and regulatory antisense mechanisms in organelles like mitochondria and chloroplasts.

The presence of ncRNAs in chloroplasts and mitochondria of a higher plant has first been demonstrated by a general analysis after cDNA cloning of small (50–500 nt) RNAs in Arabidopsis (4). Later on cloning of cDNAs corresponding to small plastid ncRNAs from tobacco revealed 11 candidates for plastids, 2 of them oriented in antisense direction to known plastid genes (5). These RNAs are very short (comprising between 19 and 53 nt) and most of them are located in intergenic regions. No function has been attributed to them until now and it cannot be excluded that at least some of them are just processing intermediates. A long antisense RNA, complementary to the reading frame of the *ndh*B gene, has been recently described. The RNA starts within the reading frame of the *ndh*B gene, the sequence covers two editing sites of the *ndh*B gene and a group II intron splice acceptor site, but no function has been attributed to this RNA, neither (6). First indication for the function of a plastid natural antisense RNA has very recently been obtained for AS5 by over-expression of the RNA *via* plastid transformation in tobacco (7). Results indicate a decrease in stability of 5S rRNA by AS5 over-expression. However, secondary effects due to plastid transformation cannot be excluded, e.g., the trangene insertion leads to the accumulation of some precursor transcripts.

In the present article, we have characterized plastid *psb*T sense/antisense RNAs. The *psb*T gene is part of the *psb*B operon (composed of *psb*B, *psb*T, *psb*H, *pet*B and *pet*D, 8) where a single gene (*psb*N) is located between the *psb*T and *psb*H genes, but on the opposite strand of the DNA (9). Transcription of the *psb*N gene is under control of sigma factor 3 (SIG3) and part of the transcription complexes proceed transcription at the end of the *psb*N gene and produce antisense RNA to the *psb*T mRNA. Only two genes seem to be specifically transcribed by SIG3-PEP holoenzyme, i.e. *psb*N and *atp*H (10). While

*To whom correspondence should be addressed. Tel: +33 (0)4 38 78 05 69; Fax: +33 (0)4 38 78 50 91; Email: silva.lerbs-mache@ujf-grenoble.fr; silva.mache@cea.fr

*psb*N is exclusively transcribed by SIG3-PEP, *atp*H is also transcribed as polycistronic RNA together with all other genes of the large ATPsynthase operon and the lack of SIG3-specific *atp*H transcription does not change the ATPH protein level (Malik Ghulam, M. *et al*., unpublished data). A SIG3 knock-out plant provides, therefore, a unique tool to elucidate the function of *psb*N initiated *psb*T antisense RNA.

The *psb*T antisense RNA is of particular interest because this antisense RNA is not restricted to the 5′ or 3′ UTR of the sense mRNA. In bacteria, ncRNAs generally base pair to mRNAs in their 5′- or 3′-UTR and the corresponding formation of RNA duplexes modifies translation efficiency and/or stability of the corresponding RNA. In the case of *psb*T, the antisense RNA covers the whole *psb*T coding region, extending at least up to the ATG translation initiation codon, as previously shown by a primer extension (PE) experiment (Figure 4B, left hand side, in 10). Furthermore, a *psb*B/*psb*T transcript had been revealed by PE having its 5′-end within the coding region of the *psb*B gene indicating either degradation of *psb*B/*psb*T co-transcripts or the possibility of decoupling of *psb*T transcription from read-through transcription of the *psb*B operon (Figure 4B, right hand side, in 10). These peculiarities stimulated us to characterize *psb*T sense and antisense RNAs in more detail with the hope to get some ideas for an eventual role of *psb*T antisense RNA in regulation of gene expression.

A mechanism in which entire genes are transcribed in sense and antisense orientation has so far been analysed in nuclear transcription where it was shown that RNA polymerase II complexes collide during transcription and stall each other or that transcription from a strong promoter hinders the transcription from a weaker promoter. This mechanism is known as 'transcriptional interference' (11,12). Regarding the high copy number of plastid genomes it is not very likely that such a mechanism exists in plastids. Also, concerning transcription of *psb*N and *psb*T, we could not detect changes in *psb*T transcript levels in *sig3* mutants, i.e. the absence of transcription from the *psb*N promoter does not change the quantity of *psb*T transcripts (Figures 3B and 4B on the right hand side, in 10). Therefore, if *psb*T sense/antisense RNA transcription is connected to any kind of regulation, it is probably not a mechanism that implies transcriptional interference.

Two types of RNA polymerase are engaged in the transcription of the plastid genome: the phage-type NEPs (nucleus-encoded plastid RNA polymerases) that are of special importance during early plant development and the eubacterial type PEP (plastid-encoded plastid RNA polymerase) that transcribes preferentially photosynthesis-related genes during later developmental stages (13,14). For correct initiation of transcription PEP needs to associate with transcription initiation factors of the sigma type (15–17) and *psb*N transcription is specifically controlled by SIG3. As none of the transcripts of the *psb*B operon changes in a *sig3* plant, we can conclude that all these RNAs are made by PEP in association with another sigma factor than SIG3 (10). Taken all together, *psb*T sense and antisense RNAs should be synthesized differently by different PEP–sigma combinations and it should be more likely that a regulatory mechanism acts *via* RNA/RNA hybrid formation than *via* transcriptional interference.

To test this hypothesis, in the present article, we have determined the 5′- and 3′-ends of *psb*T sense and antisense RNAs in order to characterize possible RNA/RNA hybrids, we have analysed whether RNA/RNA hybrids do exist and we have determined the consequence of the absence of *psb*T antisense RNA on the PSBT protein level.

MATERIALS AND METHODS

Plant material and RNA isolation

Surface-sterilized *Arabidopsis* seeds were spread on MS agar plates, kept for 72 h at 4°C in darkness and then transferred into a growth chamber and grown for 6 days at 23°C under 16/8 h light/dark cycle at 110 µmol of photons m^{-2} s^{-1}. Total RNA was prepared from seedlings as described in Privat *et al*. (18). Briefly, frozen material of plants was ground in a mortar and the powder was suspended in three volumes of solution A (10 mM Tris–HCl pH 8; 100 mM NaCl; 1 mM EDTA; 1% SDS). After two phenol–chloroform and one chloroform extractions, RNAs were separated from the bulk of DNA by precipitation in 2 M LiCl overnight and then RNAs were precipitated with ethanol.

Primer extension

The PE experiment has been performed as described in Favory *et al*. (19) using 10 µg of total RNA. Upon denaturation at 65°C, total RNAs were annealed with 100 nmol of 5′ ^{32}P-labelled primer and then retrotranscribed in the presence of 100 U of SuperScript II (Invitrogen) at 42°C according to manufacturer's protocol. RNAs were digested with 10 µg of RNase A. Before cDNAs were purified by phenol/chloroform treatment and ethanol precipitation, a ^{32}P-labelled PCR product was added to the reaction as loading control. The cDNAs were separated on a 6% polyacrylamide denaturing gel in parallel with the sequencing reaction that had been performed with the same primer. The following primers were used for PE: 5′-ATGGAAACAGCA ACCCTAGTC-3′ (*psb*N antisense, Primer 9), 5′-CATAT TGCCCTCTGACAG-3′ (*atp*I), 5′-TTCATAGTTGCAT TACT-3′ (*rrn* 16S), 5′-GATGTATCTCCTTCTCCA GG-3′ (*clp*P), 5′-GTCCAATAGAAGCAAGC-3′ (*atp*H), 5′-ATGGAAGCATTGGTTTATAC-3′ (*psb*T antisense, Primer 1).

5′-RACE

The discrimination between transcription start sites and processing sites of the *psb*T precursor RNAs was done by RNA Ligase Mediated Rapid Amplification of cDNA Ends [first choice RLM-rapid amplification of cDNA ends (RACE) kit, Ambion] without and with previous tobacco acid pyrophosphatase (TAP) treatment of RNAs. Reactions were performed according to the supplier's protocol but without removal of free 5′-phosphates

by Calf Intestine Alkaline Phosphatase. PCR products were analysed on Agarose gels after two successive PCR amplifications using at first two outer primers and the second two inner primers. Primers are as follows: *psb*T (8) 5′-GAGGCTGATTACGTTAATGAAG-3′, *psb*T (7) 5′-GAAATTTTAGGTGGTTCCCG-3′, *psb*T (6) 5′-ATC CCTAAAAGTGGATACTAAGAG-3′, *psb*T (5) 5′-GAG TCAAAGAAACGGCAGCG-3′. The inner and outer adapter primers are those of the RLM-RACE Kit.

Circular RT–PCR

In order to map the extremities of the *psb*T antisense transcripts, the first choice RLM-RACE kit (Ambion) was used. Total RNAs were first incubated with TAP and then self-ligated. About 400 ng of RNAs were retro-transcribed using Primer (2) 5′-ATGGAAGCATT GGTTTATAC-3′ as gene-specific primer and the SuperScript II enzyme. Subsequent PCR amplification was performed in the presence of primer (3) 5′-ATCCCT AAAGTGGATACTAAG-3′ and primer (4) 5′-CGGGA ACCACCTAAAATTTCAAC-3′. Reactions without TAP and without RT reaction were carried out as controls. The produced cDNAs have been cloned into pCR^{R}2.1-TOPO vector using the TOPO TA cloning kit (Invitrogen) and sequenced.

Antibody production and characterization

Antibodies against the PSBB and PSBH proteins of Photosystem II (PSII) have been obtained from Agrisera. Antibodies against nucleus-encoded plastid ribosomal protein L4 have been described earlier (20). Peptide antibodies against PSBT have been produced by Eurogentec using the following peptide: AIFFREPPKIS TKK.

Protein purification and western blot analysis

A 200 mg of plant material were frozen-grounded and resuspended in 200 µl of protein loading dye. After boiling for 10 min, protein extracts were cleared by full speed-centrifugation in a micro-centrifuge. Equal amounts of protein extracts were separated by SDS–PAGE and transferred to nitrocellulose membranes. For immunodetection antibodies were diluted 1 : 1000 (PSBT), 1 : 5000 (PSBH) and 1 : 2000 (PSBB) and revealed by the ECL detection kit (GE Healthcare).

Characterization of double-stranded RNA

Total RNA has been treated with DNase (Ambion) according to the manufacturer's instructions until no traces of DNA could be detected by PCR analysis. DNA-free total RNA (1 µg) has been digested with Nuclease S1 at different concentrations (28) at room temperature for 30 min. Nuclease S1 was inactivated by addition of EDTA (final concentration 1.6 mM) and incubation at 75°C for 15 min. Reverse transcription of the different mRNAs was carried out using 100 ng RNA from the Nuclease S1 assay, SuperScript II (Invitrogen) and gene-specific primers according to the manufacturer's protocol. A 1 µl of the cDNA reaction was taken for further PCR amplification using Primer 1 and Primer 5′-GAGGCTGATTACGTTA ATG-3′ for *psbT* amplification and Primers 5′-TGATATT ATGGATGACTGGTTACGG-3′ and 5′-TGCAACCTT CTAAATAGGAACTGG-3′ for *psbD* amplification.

RESULTS

Mapping of 3′-ends of *psb*T antisense transcripts

By using a primer that starts at the ATG translation initiation codon of the *psb*T gene, we have recently mapped the 5′-end of the *psb*T antisense transcript by PE. We have shown that the *psb*T antisense RNA arises from a long P*psb*N initiated transcript that is cleaved in the intergenic region between *psb*T and *psb*N (10). This cleavage that provides the 5′-end of the *psb*T antisense RNA is illustrated in Figure 1A. The dotted line represents the P*psb*N initiated transcript and the cleavage site is indicated by the vertical open arrow with the scissor (PE, 1).

In order to determine now the 3′-end(s) of the *psb*T antisense transcript, we performed circular RT–PCR (cRT–PCR) analyses (21). The principle of the method is schematized on the left hand side in Figure 1B. After joining 5′- and 3′-ends of the RNAs by treatment with RNA ligase, circularized RNAs have been reverse transcribed using Primer 2 and the produced cDNAs have been PCR amplified with Primers 3 and 4. The sequences surrounding the 5′ and 3′ joining points reveal the 5′- and 3′-ends of the antisense RNAs. The reaction resulted in two different PCR products (Figure 1B, right hand side) indicating the existence of two different antisense RNAs. The sequencing of both PCR products showed that both antisense RNAs have the same 5′-end corresponding to the 5′-end of the *psb*T antisense RNA as determined previously by PE using Primer 1 (10 and Figure 1A). However, the 3′-ends are different. The 3′-end of the 'a' transcript is situated within the coding region of the *psb*B gene and the 3′-end of the 'b' transcript is located in the intergenic region between *psb*B and *psb*T. The sequences at the 3′-ends of the 'a' and the 'b' antisense RNAs are reported in Figure 1C.

Mapping of 5′-ends of *psb*T sense transcripts

Our previous PE experiment had revealed two different *psb*T transcripts, one with a 5′-end located in the intergenic region between *psb*T and *psb*B and a longer transcript with a 5′-end positioned within the *psb*B coding region (10). These transcripts are reported by dotted lines in Figure 2A (Primer 7, PE). From the PE experiment, it was not clear whether these RNAs are made by transcription initiation or by processing of a P*psb*B-initiated multicistronic mRNA. To answer this question, we have performed 5′-RACE experiments with and without prior treatment of RNAs with TAP. By using either Primers 7 and 6 or Primers 8 and 6 (for primer localization see Figure 2A), we obtained a single-PCR product, and this product was only obtained after TAP treatment showing that this transcript is made by transcription initiation (Figure 2B). The corresponding cDNA has been cloned and sequenced and the location

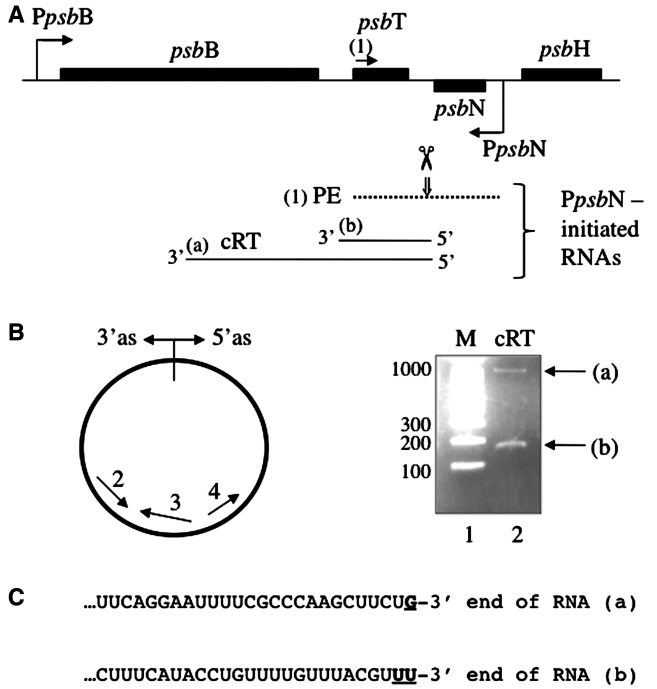

Figure 1. Determination of 3′-ends of *psb*T antisense RNAs. (**A**) Schematic representation of a part of the *psb*B operon and the *psb*T antisense transcripts. The dotted line indicates the 5′-end of P*psb*N initiated RNA as determined previously (10) by PE using Primer 1. The localization of the primer is marked in the presentation of the *psb*B operon by a short horizontal arrow. The uninterrupted lines (a and b) reveal *psb*T antisense RNAs as determined by ligation-mediated circular RT–PCR (cRT). (**B**) The method of circular RT–PCR is schematically demonstrated (left) and the two obtained cDNAs [(a) and (b)] are shown on the right hand side after separation on an agarose gel (Lane 2). M represent the co-migrated molecular weight markers (Lane 1). (**C**) Nucleotide sequences at the 3′-ends of the two antisense RNAs (a) and (b) as determined by cRT. 3′-ends are indicated by bold and underlined letters.

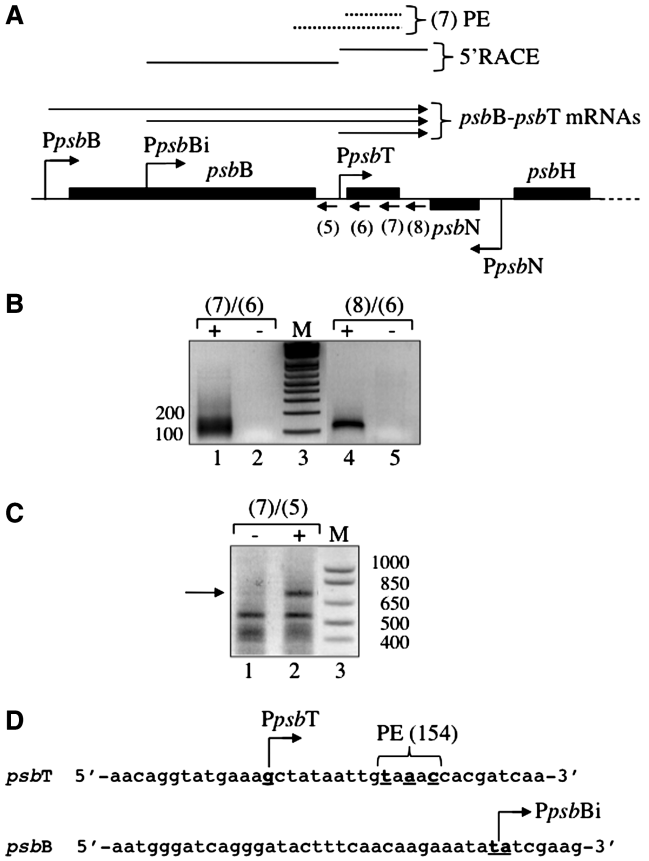

Figure 2. Determination of 5′-ends of *psb*T sense RNAs. (**A**) Schematic representation of a part of the *psb*B operon and the *psb*T sense transcripts. The short horizontal arrows labelled (5)–(8) show the localization of the primers that have been used in PE and/or 5′-RACE experiments. The dotted lines represent *psb*T transcripts that had been previously identified by PE using Primer 7. The two uninterrupted lines correspond to the two cDNAs revealed by 5′-RACE as shown in B and C. The three long horizontal arrows indicate the existence of three *psb*T transcripts that are initiated at three different promoters, P*psb*B, P*psb*Bi or P*psb*T. (**B**) Agarose electrophoresis of 5′-RACE cDNAs of *psb*T RNAs obtained by using Primers 7 and 6 (LANE 1) or Primers 8 and 6 (Lane 4). Lanes 3 and 5 represent reactions in which RNAs have not been treated with TAP before ligation. M shows molecular weight standards. (**C**) Electrophoretic separation of *psb*T RNA 5′-RACE products obtained by using Primers 7 and 5 with (+, Lane 2) and without (−, Lane 1) TAP treatment. M corresponds to molecular weight standards indicated in base pair at the right hand side of the figure. (**D**) Nucleotide sequence surrounding the two transcription start sites, P*psb*T and P*psb*Bi. The cleavage site(s) of the P*psb*T initiated RNA as determined previously by PE (10) are underlined and marked PE (154).

of the transcription start site, in the intergenic region between *psb*B and *psb*T, is indicated in Figure 2D as P*psb*T.

When compared with our previous result obtained by PE (labelled as 154 RNAs in Figure 4B and C, in 10 and in Figure 2D), we realize a small difference between the 5′-ends as revealed by PE and by 5′-RACE. We interpret this difference by rapid nucleolytic removal of the first 9/10 nt at the 5′-end of the P*psb*T-initiated mRNA immediately after synthesis. This is in agreement with the fact that PE experiments always showed several cDNAs of slightly different length, a fact that indicates nucleolytic attack at the 5′-end. An explanation for the sensitivity to nucleolytic digestion of the P*psb*T-initiated mRNA at its 5′-end is provided by the secondary structure of this RNA (Supplementary Figure S1). It shows formation of a hairpin at the 5′-end of the mRNA that does not include the nucleotides between positions P*psb*T and (154) (Figure 2D). This hairpin structure might stabilize the 5′-end of the *psb*T mRNA and protect the mRNA from further nuclease digestion. This structure might also explain why we did not detect the shorter transcripts by 5′-RACE. Probably, ligation will not be successful on 5′-ends that are base-paired within a hairpin structure.

For exact mapping of the 5′-end of the longer *psb*T transcript that is located within the coding region of the *psb*B gene (Figure 2A, dotted lines, 7 PE), we needed to use an inner primer that is located close to the *psb*B gene (Primer 5 in Figure 2A). 5′-RACE shows the existence of several RNAs and only one of them is made by transcription initiation (Figure 2C). This transcript is much longer than that expected for the PE product. Cloning of the corresponding cDNA revealed a promoter that is located within the coding region of the *psb*B gene. The sequence surrounding this transcription start site is shown in Figure 2D. The other cDNAs of the 5′-RACE

experiment that do not result from transcription initiation indicate the existence of several cleavage intermediates of the *psb*B mRNA. These have not been further analysed. The results obtained here indicate the existence of two different *psb*B/*psb*T co-transcripts, one initiating at P*psb*B and the other one initiating at P*psb*Bi (Figure 2A). The length of these two transcripts correspond well to the two RNAs of about 2000 and 1000 bases that have been revealed by Northern hybridization in our previous paper (10).

Mapping of the 3′-end of the *psb*T sense transcript

In order to get an idea of the 3′-end of the *psb*T sense transcripts, we next analysed the *psb*T/*psb*H intergenic region by PE. This should reveal the 5′-end of the cleavage product of the *psb*T/*psb*H co-transcript (Figure 3). We used a primer that was located at the beginning of the *psb*N gene as indicated in Figure 3A (Primer 9). To test whether the absence of antisense RNA influences the processing in the *psb*T–*psb*H intergenic region, we analysed RNA prepared from wild type (WT) the *SIG3* knockout mutant (Δ3) in this experiment. We observed three different cDNAs, labelled with (a) and (*) in Figures 3A and B. All three cDNAs are also found in the *sig3* plants (compare Lanes 5 and 6 in Figure 3B) showing that the corresponding processing events are not disturbed by the absence of antisense RNA. The 5′-end of the shortest RNA could be localized with the accompanying sequence ladder. It is positioned within a perfect hairpin structure that could form within the intergenic region between *psb*T and *psb*N. The exact location in the nucleic acid sequence is reported in Figure 3C. Interestingly, the 5′-end of the *psb*T antisense RNA that had been determined by cRT–PCR (Figure 1A) and by PE (10) is located in the complementary hairpin (labelled with PE and cRT in Figure 3C). The two longer transcripts (asterisks) have not been observed in all RNA preparations and have not been mapped.

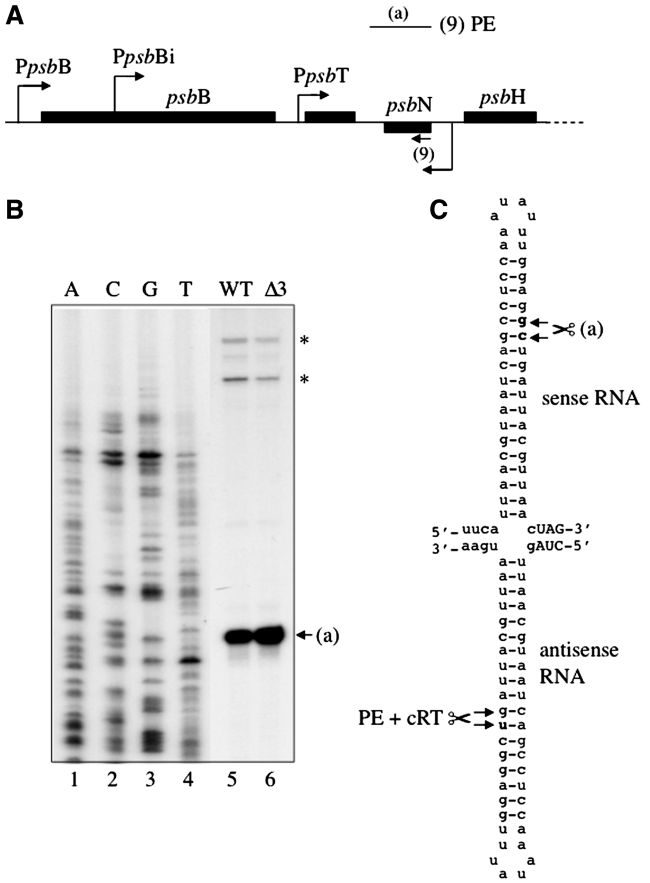

Figure 3. Mapping of the 3′-end of the *psb*T sense transcript. (**A**) Schematic representation of a part of the *psb*B operon and *the psb*N antisense transcript (a) as determined by PE using Primer 9. The horizontal arrow indicates the localization of the primer. (**B**) PE analysis of *psb*N antisense RNA performed with Primer 9. The accompanying sequence ladder has been established by using the same primer. The revealed cDNA (a) is schematically demonstrated in (A). (**C**) Localization of the cleavage sites of *psb*T sense/*psb*N antisense (upper hairpin) and *psb*N sense/*psb*Tantisense RNAs (lower hairpin).

Characterization of sense/antisense double-stranded RNAs

Our mapping of 5′- and 3′-ends of *psb*T sense and antisense RNAs offers several possibilities for RNA/RNA hybrid formation. The 3′-ends of the sense and antisense RNAs are well defined and seemed to be stable. Equally, the 5′-end of the antisense RNA could be determined with precision. However, the 5′-end(s) of the *psb*T sense RNAs that comprise part of the *psb*B coding region are divers and multiple degradation intermediates seem to exist (Figure 2C). The two most likely possibilities of sense/antisense hybrids are schematized in Figure 4A. We assume that P*psb*Bi initiated transcripts that are not protected by hybrid formation will be degraded from the 5′-end and this gives rise to the degradation intermediates that we observe in Figure 2C. The complete RNA sequences of the short *psb*T sense/antisense RNA hybrid are shown in Figure 4B. The estimated location of a chloroplast ribosome on the single-stranded *psb*T sense mRNA as deduced from the work of Kim and Mullet (22) is indicated by the open circle above the sequence. It shows that the single-stranded mRNA could be protected from 5′ nucleolytic attack by an initiating ribosome, but only up to the 5′-end that had been revealed by PE (vertical flashes on the sequence). The first 10 nt of the P*psb*T-initiated mRNA would not be protected by an initiating ribosome. Thus, in addition to the secondary structure of free *psb*T mRNA (see Supplementary Figure S1) initiating ribosomes could also protect the 5′-end from degradation, except for the first 10 nt.

Do *psb*T RNA sense/antisense hybrids exist *in vivo*?

Having shown the existence of *psb*T sense and antisense transcripts, it was of interest to know whether RNA/RNA double strands do indeed form *in vivo*. This question was examined by treating total RNA with the single-strand-specific nucleases Nuclease S1. If sense/antisense RNA hybrids exist the RNAs that are engaged in hybrid structures should be protected from nuclease digestion. In contrast, mRNA that is not protected by antisense RNA should be totally degraded.

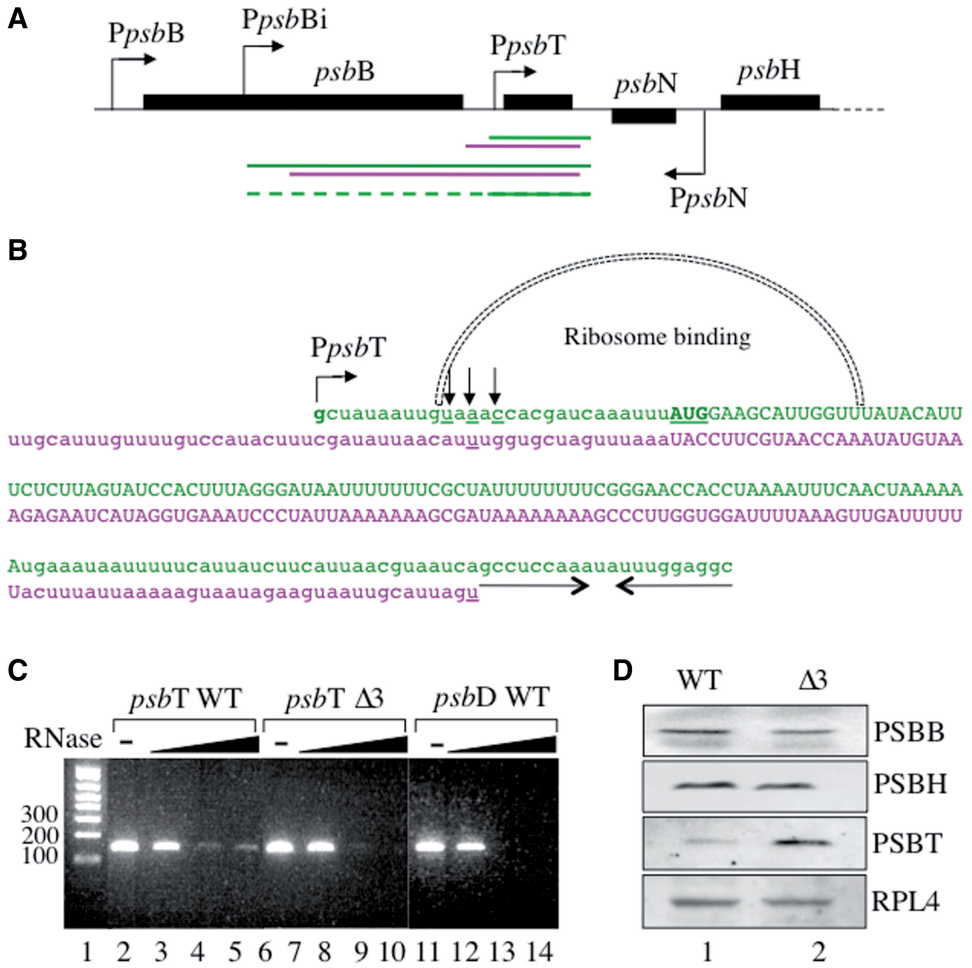

Figure 4. Characterization of *psb*T sense/antisense double-stranded RNAs and the influence of double-strand formation on the PSBT protein level. (**A**) Schematic representation of a part of the *psb*B operon and possible *psb*T sense (green)/antisense (magenta) double-stranded RNAs. The dotted line indicates supposed 5′ nucleolytic degradation of single-stranded sense RNA. (**B**) Nucleotide sequence of the short *psb*T sense (green)/antisense (magenta) hybrid. Vertical arrows label 5′ *psb*T cleavage sites. The 3′ overhanging part of the *psb*T sense RNA corresponds to an inverted repeat as indicated by two opposite horizontal arrows. Ribosome binding on single-stranded *psb*T mRNA is simulated by half of a circle. (**C**) RT–PCR amplification of *psb*T mRNA in 7 days old WT (Lanes 2–5) and *sig3* plantlets (Lanes 6–10) and *psbD* mRNA in WT plantlets (Lanes 11–14) without (Lanes 2, 6 and 11) and after digestion with either 0.02 U/µl (Lanes 3, 7 and 12), 0.2 U/µl (Lanes 4, 8 and 13) or 2 U/µl (Lanes 5, 10 and 14) of Nuclease S1. Lane 1 corresponds to molecular weight standards. (**D**) Western immunoblot analyses of total protein extracts prepared from WT (Lane 1) and *sig3* (Lane 2) plants by using antibodies made against PSBB, PSBH, PSBT and RPL4 proteins.

We have analysed *psb*T mRNA in WT and *sig*3 plants and *psb*D mRNA in WT plants taken as control without and after treatment with several concentrations of Nuclease S1 (Figure 4C). The *psb*D control mRNA was no more detectable when the nuclease concentration was 0.2 U/µl or higher (Lanes 11–14). In WT plants the *psb*T mRNA level diminishes after treatment with 0.2 U/µl of nuclease, but then remains stable even after treatment with a 10× higher nuclease concentration (Lanes 2–5). In contrast, in the *sig*3 mutant the *psb*T mRNA disappears completely after high nuclease treatment (Lanes 6–10). This result strongly suggests that p*sb*T sense/antisense hybrids exist *in vivo*.

Functional characterization of *psb*T sense/antisense hybrids

The question of the function of the *psb*T antisense RNA can best be analysed by using the *SIG3* knockout mutant. In the absence of SIG3 the *psb*N gene is not transcribed and *psb*T antisense RNA cannot be produced. In the following, we have analysed the protein levels of PSBT and of the adjacently encoded PSBB and PSBH proteins in WT and *ΔSIG3* plants (Figure 4D). The amount of the nucleus-encoded plastid ribosomal protein L4 has been analysed as loading control. In the absence of *psb*T antisense RNA, we observe a remarkable augmentation of the PSBT protein level. This augmentation is restricted to PSBT. The PSBB and PSBH protein levels are not influenced by the absence of *psb*T antisense RNA. This result can be interpreted in that *psb*T mRNA that is engaged in a sense/antisense double-stranded RNA hybrid cannot be translated. In the absence of antisense RNA, the quantity of translation competent free single-stranded *psb*T RNA increases and more PSBT protein can be produced.

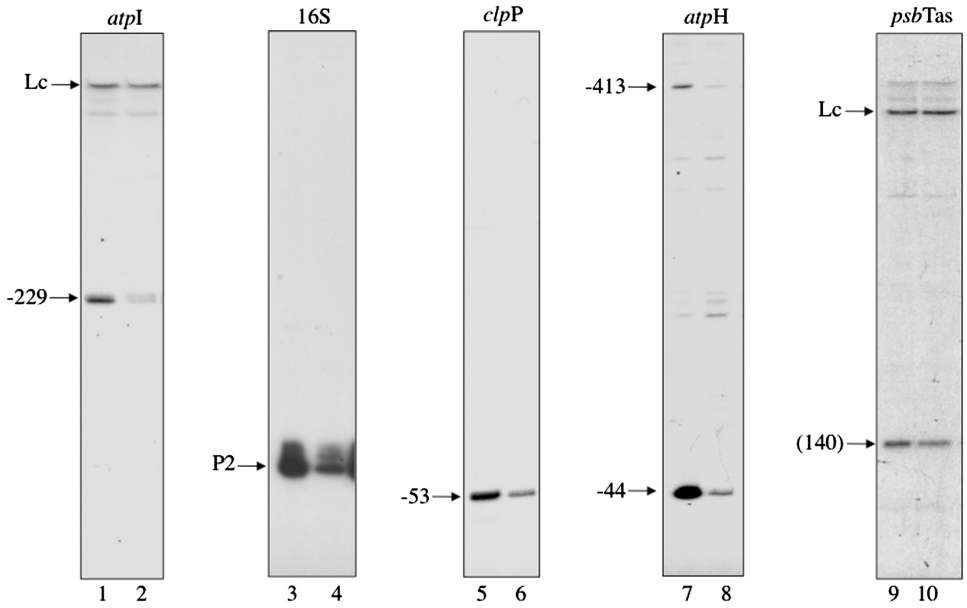

Figure 5. Analysis of different mRNA levels in response to photooxydative stress. *Arabidopsis* plantlets grown under 110 µE light intensity and 16/8 h light/dark cycle were either kept at 110 µE for additional 4 h (Lanes 1, 3, 5, 7 and 9) or exposed to 1300 µE for 4 h (Lanes 2, 4, 6, 8 and 10). After extraction of total RNA precursor RNAs of *atp*I (Lanes 1 and 2), *16S* ribosomal RNA (Lanes 3 and 4), *clp*P (Lanes 5 and 6) and *atp*H (Lanes 7 and 8) were analysed by PE. Lanes 9 and 10 show PE products of *psb*T antisense RNA for comparison. The *atp*H, *clpP* and *psb*Tas transcipts are labelled as in Zghidi *et al.* (10). P2 corresponds to the *rrn*-P2 promoter and −53 to the major *clp*P transcript. Lc represents an 800 bp PCR-amplified radiolabelled DNA fragment that has been added as loading control to the reaction after reverse transcription.

DISCUSSION

We have recently shown that SIG3-PEP-specific transcription initiation at the plastid *psb*N gene produces antisense RNA to the *psb*T mRNA (10). In these experiments, antisense RNA was revealed by PE using a primer that corresponds to the 5′-end of the *psb*T mRNA and the result showed that the antisense RNA covers the entire coding region of the *psb*T mRNA. In the present article, we have characterized the *psb*T sense and antisense RNAs in more detail. The determination of RNA 5′- and 3′-ends by either 5′-RACE or cRT–PCR indicates the existence of two different sense and antisense RNAs, one covering only the *psb*T gene area and the other, longer, one covering in addition a large part of the *psb*B-coding region (Figures 1–3).

The existence of these four different RNAs offers in principal four different possibilities of RNA/RNA hybrid formation. Only the two more likely to occur in a stable form are schematized in Figure 4A. Hybridization of a short with a long RNA cannot be excluded, but it would leave a large part of the long RNA in single-stranded form, more easily susceptible to nucleolytic degradation. Indeed, a long *psb*T sense RNA seems to be subject to extensive 5′ degradation. This is indicated by the existence of multiple intermediary RNAs as shown in Figure 2C. However, it is not possible to distinguish degradation products of P*psb*B initiated transcripts from degradation products of P*psb*Bi initiated transcripts. In principle, antisense RNA could also hybridize with P*psb*B-initiated mRNA. However, in this case, double-strand formation should interfere with *psb*B mRNA translation and we should have found an increase of the PSBB protein level in the absence of antisense RNA in the western experiment (Figure 4D). As this is not the case, our results rather indicate that all long antisense RNA is sequestered in double strands by hybridization with P*psb*Bi initiated sense transcripts. The absence of antisense RNA could then liberate the P*psb*Bi initiated sense transcripts that might be either degraded or translated from the *psb*T ATG translation start codon. Another explanation would consist in that the long *psb*T/*psb*B antisense RNA is present in a very low amount and its absence does not change the PSBT protein level.

If we regard now, the short sense/antisense RNAs, we see that after formation of the double-strand ribosome association to the sense *psb*T RNA should be impeded (Figure 4B) and the RNA should not be translatable. Translatable *psb*T mRNA should be liberated in the absence of antisense RNA. This hypothesis seems to be proven by the analysis of the PSBT protein in WT and *sig3* plants that shows a considerable increase of the protein in the absence of antisense RNA (Figure 4D). From this result, it becomes clear that differences in the amount of *psb*T antisense RNA will influence the PSBT protein level. *Psb*T sense transcripts are under control of other sigma factors than *psb*N/*psb*T antisense transcripts. This fact provides impact for differential expression of sense and antisense RNAs and consequently for regulation of *psb*T gene expression by antisense RNA. Nevertheless, the question of the physiological meaning of such antisense RNA regulation remains open.

To approach this question, we need to consider the production and the function of the *psb*T protein. Actually, there are three different hypotheses for the function of PSBT. (i) PSBT is required for efficient repair of

photodamaged PSII reaction centres (23), (ii) PSBT plays an important role in dimerization of PSII (24) and (iii) PSBT is required for efficient biogenesis of PSII complexes (25). Interestingly, the crystal structure of PSII shows that PSBT is localized at the PSII dimer interface, consistent with a role in dimerization (26). The kinetics of protein accumulation during greening is different for PSBT when compared with other PSII proteins and the absence of PSBT does not affect the synthesis of other PSII proteins (25). This indicates that PSBT synthesis is differently regulated than other PSII proteins. The mechanisms of this regulation are not known, but it is tempting to speculate that *psb*T expression is at least partly regulated by an antisense RNA pathway.

In principal, the production of antisense RNA could help to diminish the *psb*T protein level under some physiological conditions. Our results show that antisense transcription diminishes the level of PSBT protein (Figure 4D). However, diminution of sense RNA availability for translation as prevailing mechanisms of antisense RNA production does not make much sense with regard to the two promoters that are found upstream of the *psb*T gene (Figure 2). Another possible function of the antisense RNA might be protection of the sense RNA from nucleolytic degradation under some adverse physiological conditions. That *psb*T sense/antisense RNA hybrids do really exist *in vivo* is shown in Figure 4C and RNA/RNA hybrids are known to be very stable (27). Furthermore, a protecting effect against mRNA 3′-end degradation by antisense RNA has already been shown in chloroplasts of *Chlamydomonas* (28). As already mentioned, PSBT is required for repair of photodamaged PSII reaction centres (27). To get a first idea whether mRNA protection might be necessary during photooxydative stress, we have analysed several mRNAs by PE before and after exposure of 7-day old normally grown *Arabidopsis* plantlets to high light condition (1300 µE) for 4 h (Figure 5). We have analysed *atp*I (Lanes 1 and 2), 16S (Lanes 3 and 4) and *atp*H (Lanes 7 and 8) precursor RNAs as examples for PEP transcripts and *clp*P (Lanes 5 and 6) precursor RNA as example for a NEP transcript. In all cases, transcript levels diminish strongly after exposure to high light indicating rapid degradation of all these mRNAs under light stress conditions. An exception represents the *psb*T antisense RNA for which the RNA level remains rather stable (Lanes 9 and 10). If *psb*T antisense RNA is protected from nucleolytic attack by double-strand formation with *psb*T sense RNA, the part of the *psb*T sense RNA that is sequestered in the double strand, should also be protected from degradation. Consequently, the amount of *psb*T antisense RNAs could determine the amount of *psb*T sense RNA that is protected during photooxydative stress. Such a mechanism raises the question of how the sense RNA is made available for translation after the stress.

Altogether, our results suggest two possible functions for *psb*T antisense RNA: inhibition of translation of sense RNA and/or protection of sense RNA from nucleolytic degradation during stress conditions. Both mechanisms might not be mutually exclusive. Although the here presented results do not yet reveal the exact function of the *psb*T antisense RNA for *psb*T gene expression they provide solid impact for further analyses.

SUPPLEMENTARY DATA

Supplementary Data are available at NAR Online.

FUNDING

The Centre National de la Recherche Scientifique and the French Ministry of Education; Société française d'exportation des ressources éducatives (to M.M.G.); FLORALIS (to F.B.). Funding for open access charge: The Centre National de la Recherche Scientifique.

Conflict of interest statement. None declared.

REFERENCES

1. Lapidot,M. and Pilpel,Y. (2006) Genome-wide natural antisense transcription: coupling its regulation to its different regulatory mechanisms. *EMBO Reports*, **7**, 1216–1222.
2. Werner,A. and Swan,D. (2010) What are natural antisense transcripts good for? *Biochem. Soc. Transact*., **38**, 1144–1149.
3. Repoila,F. and Darfeuille,F. (2009) Small regulatory non-coding RNAs in bacteria: physiology and mechanistic aspects. *Biol. Cell*, **101**, 117–131.
4. Marker,C., Zemann,A., Terhörst,T., Kiefmann,M., Bachellerie,J.P., Brosius,J. and Hüttenhofer,A. (2002) Experimental RNomics: Identification of 140 candidates for small non-messenger RNAs in the plant Arabidopsis thaliana. *Curr. Biol*., **19**, 2002–2013.
5. Lung,B., Zemann,A., Madej,M.J., Schuelke,M., Techritz,S., Ruf,S., Bock,R. and Hüttenhofer,A. (2006) Identification of small non-coding RNAs from mitochondria and chloroplasts. *Nucleic Acids Res*., **34**, 3842–3852.
6. Georg,J., Honsel,A., Voss,B., Rennenberg,H. and Hess,W.R. (2010) A long antisense RNA in plant chloroplasts. *New Phytologist*, **186**, 615–622.
7. Hotto,A.M., Huston,Z.E. and Stern,D.B. (2010) Overexpression of a natural chloroplast-encoded antisense RNA in tobacco destabilizes 5S rRNA and retards plant growth. *BMC Plant Biol*., **10**, 213.
8. Westhoff,P. and Herrmann,R.G. (1988) Complex RNA maturation in chloroplasts: the *psb*B operon from spinach. *Eur. J. Biochem*., **171**, 551–564.
9. Kohchi,T., Yoshida,T., Komano,T. and Ohyama,K. (1988) Divergent mRNA transcription in the chloroplast *psbB* operon. *EMBO J*., **7**, 885–891.
10. Zghidi,W., Merendino,L., Cottet,A., Mache,R. and Lerbs-Mache,S. (2007) Nucleus-encoded plastid sigma factor SIG3 transcribes specifically the *psb*N gene in plastids. *Nucleic Acids Res*., **35**, 455–464.
11. Hongay,C.F., Grisafi,P.L., Galitski,T. and Fink,G.R. (2006) Antisense transcription controls cell fate in Saccharomyces cerevisiae. *Cell*, **127**, 735–745.
12. Yazgan,O. and Krebs,J.E. (2007) Non-coding but non-expendable: transcriptional regulation by large non-coding RNA in eukaryotes. *Biochem. Cell Biol*., **85**, 484–496.
13. Shiina,T., Tsunoyama,Y., Nakahira,Y. and Khan,M.S. (2005) Plastid RNA Polymerases, Promoters, and Transcription Regulators in Higher Plants. *Int. Rev. Cytol*., **244**, 1–68.
14. Liere,K. and Börner,T. (2006) Transcription of plastid genes. In Grasser,K.Q. (ed.), *Regulation of Transcription in Plants*. Blackwell Publishing Ltd., Oxford, pp. 184–224.
15. Lysenko,E.A. (2007) Plant sigma factors and their role in plastid transcription. *Plant Cell Rep*., **26**, 845–859.

16. Schweer,J. (2010) Sigma factors come of age: flexible transcription factor network for regulated plastid gene expression. *Endocytobiosis Cell Res.*, **20**, 1–20.
17. Lerbs-Mache,S. Function of plastid sigma factors in higher plants: regulation of gene expression or just preservation of constitutive transcription? *Plant Mol. Biol.*, doi:10.1007/s11103-010-9714-4.
18. Privat,I., Hakimi,M.A., Buhot,L., Favory,J.J. and Lerbs-Mache,S. (2003) Characterization of Arabidopsis plastid sigma-like transcription factors SIG1, SIG2 and SIG3. *Plant Mol. Biol.*, **55**, 385–399.
19. Favory,J.J., Kobayshi,M., Tanaka,K., Peltier,G., Kreis,M., Valay,J.G. and Lerbs-Mache,S. (2005) Specific function of a plastid sigma factor for *ndh*F gene transcription. *Nucleic Acids Res.*, **33**, 5991–5999.
20. Trifa,Y., Privat,I., Gagnon,J., Baeza,L. and Lerbs-Mache,S. (1998) The nuclear *RPL4* gene encodes a chloroplast protein that co-purifies with the T7-like transcrption complex as well as plastid ribosomes. *J. Biol. Chem.*, **273**, 3980–3985.
21. Perrin,R., Meyer,E.H., Zaepfel,M., Kim,Y.J., Mache,R., Grienenberger,J.M., Gualberto,J.M. and Gagliardi,D. (2004) Two exoribonucleases act sequentially to process mature 3′-ends of atp9 mRNAs in Arabidopsis mitochondria. *J. Biol. Chem.*, **279**, 25440–25446.
22. Kim,J. and Mullet,J.E. (1994) Ribosome-binding sits on chloroplast rbcL and psbA mRNAs and light-induced initiation of D1 translation. *Plant Mol. Biol.*, **25**, 437–448.
23. Ohnishi,N., Kashino,Y., Satoh,K., Ozawa,S.I. and Takahashi,Y. (2007) Chloroplast-encoded polypeptide PsbT is involved in the repair of primary electron acceptor QA of photosystem II during photoinhibition in *Chlamydomonas reinhardtii*. *J. Biol. Chem.*, **282**, 7107–7115.
24. Iwai,M., Katoh,H., Katayama,M. and Ikeuchi,M. (2004) PSII-Tc protein plays an important role in dimerisation of photosystem II. *Plant Cell Physiol.*, **45**, 1809–1816.
25. Ohnishi,N. and Takahashi,Y. (2008) Chloroplast-encoded PsbT is required for efficient biogenesis of photosystem II complex in the green alga *Chlamydomonas reinhardtii*. *Photosynth. Res.*, **98**, 315–322.
26. Guskov,A., Kern,J., Gabdulkhakov,A., Broser,M., Zouni,A. and Saenger,W. (2009) Cyanobacterial photosystem II at 2.9-A resolution and the role of quinones, lipids, channels and chloride. *Nat. Struct. Mol. Biol.*, **16**, 334–342.
27. Sugimoto,N., Nakano,S., Kato,M., Matsumara,A., Nakamuta,H., Ohmichi,T., Yoneyama,M. and Sasaki,M. (1995) Thermodynamic parameters to predict stability of RNA/DNA hybrid duplexes. *Biochemistry*, **34**, 11211–11216.
28. Nishimura,Y., Kikis,E.A., Zimmer,S.L., Komine,Y. and Stern,D.B. (2004) Antisense transcript and RNA processing alterations suppress instability of polyadenylated mRNA in Chlamydomonas chloroplasts. *Plant Cell*, **16**, 2849–2869.